Dehydration behavior of the superprotonic conductor CsH_2PO_4 at moderate temperatures: 230 to 260 °C†

Yu-ki Taninouchi,[a] Tetsuya Uda,*[a] Yasuhiro Awakura,[a] Ayako Ikeda[b] and Sossina M. Haile[b]

Received 26th March 2007, Accepted 16th May 2007
First published as an Advance Article on the web 1st June 2007
DOI: 10.1039/b704558c

The dehydration behavior of caesium dihydrogen phosphate CsH_2PO_4 was investigated in the temperature range of 230 °C to 260 °C under high humidity, conditions of particular relevance to the operation of fuel cells based on this electrolyte. The onset temperature of dehydration was determined from changes in ionic conductivity on heating and confirmed by weight change measurements under isothermal conditions. The relationship between the onset temperature of dehydration (T_{dehy}) and water partial pressure (p_{H_2O}) was determined to be $\log(p_{H_2O}/\text{atm} = 6.11(\pm 0.82) - 3.63(\pm 0.42) \times 1000/(T_{dehy}/\text{K})$, from which the thermodynamic parameters of the dehydration reaction from CsH_2PO_4 to $CsPO_3$ were evaluated. The dehydration pathway was then probed by X-ray powder diffraction analysis of the product phases and by thermogravimetric analysis under slow heating. It was found that, although the equilibrium dehydration product is solid caesium metaphosphate $CsPO_3$, the reaction occurs *via* two overlapping steps: $CsH_2PO_4 \rightarrow Cs_2H_2P_2O_7 \rightarrow CsPO_3$, with solid caesium hydrogen pyrophosphate, $Cs_2H_2P_2O_7$, appearing as a kinetically favored, transient phase.

1. Introduction

Caesium dihydrogen phosphate (CsH_2PO_4) belongs to a group of compounds that have properties intermediate between those of a normal salt and an acid, and it undergoes a transition from a paraelectric phase to a superprotonic phase at *ca.* 228 °C.[1–4] The superprotonic phase of CsH_2PO_4 exhibits proton conductivity greater than 10^{-2} S cm^{-1}, and stable operation of fuel cells using this material as the electrolyte has been recently reported.[5] In addition, fabrication routes for obtaining competitive power densities have been demonstrated,[6] as has effective direct utilization of alcohol fuels.[7] A unique feature of CsH_2PO_4 electrolyte fuel cells (solid acid fuel cells, SAFCs) is their operability at intermediate temperatures of around 250 °C. Anticipated benefits of fuel cell operation at intermediate temperatures include a high probability of discovering platinum-free catalysts, the possibility of utilizing waste heat, and compatibility with low-cost structural materials such as stainless steel.

Despite these advantages, several challenges underlie the practical implementation of SAFCs. Key amongst these is the dehydration/decomposition of CsH_2PO_4 at temperatures above *ca.* 200 °C, precisely the temperatures required to obtain high conductivity. This dehydration can be suppressed by maintaining sufficient water partial pressure in the fuel cell system. However, implementing this relatively straightforward solution requires precise knowledge of the thermodynamics of the dehydration process. To date, only a few preliminary studies of the relationship between the onset temperature of dehydration and the partial pressure of water have been reported.[5,8] From a fundamental perspective, it is also of value to elucidate the dehydration pathway, particularly since dehydration has been argued by some to play a role in the high conductivity of the superprotonic phase.[9] Moreover, there is some controversy regarding the nature of the final product phase. While some researchers have reported that CsH_2PO_4 dehydrates under dry or vacuum conditions[10,11] to ultimately yield caesium metaphosphate ($CsPO_3$), others have observed caesium hydrogen pyrophosphate ($Cs_2H_2PO_7$) upon dehydration under air,[3,12] and none have reported the behavior under suitably humidified conditions. This situation further motivates a study of the dehydration pathway.

In this work, we investigate the dehydration behavior of CsH_2PO_4 under essentially practical conditions, *i.e.*, in the SAFC-operating temperature range of 230 °C to 260 °C. The onset of dehydration is probed by measuring changes in ionic conductivity on heating, as well as by isothermal weight change measurements. Thermogravimetric analysis (TGA) under slow heating and X-ray diffraction (XRD) analysis of the product phases are then employed to provide insight into the dehydration reaction pathway. The results are subsequently analyzed to determine thermodynamic parameters of the dehydration reaction.

2. Material synthesis and characterization

CsH_2PO_4 was prepared from an aqueous solution of Cs_2CO_3 and H_3PO_4, in which the amount of H_3PO_4 was slightly higher than that required by the stoichiometry of the desired phase.[4,13] Polycrystalline powder of CsH_2PO_4 was precipitated

[a]*Department of Materials Science and Engineering, Kyoto University, Sakyo, Kyoto 606-8501, Japan*
[b]*Department of Materials Science, California Institute of Technology, 1200 California Blvd, Pasadena, CA 91125, USA.*
E-mail: tetsuya-uda@mtl.kyoto-u.ac.jp; Fax: +81-75-753-5284; Tel: +81-75-753-5445

† This paper is part of a *Journal of Materials Chemistry* theme issue on New Energy Materials. Guest editor: M. Saiful Islam.

by introduction of methanol into the solution. The resulting powder was filtered, washed using methanol or toluene, and finally dried at 125 °C. The XRD pattern of the powder showed that phase pure CsH_2PO_4 had been obtained.[14] The typical particle size was in the range of 2 to 80 μm. In addition, chemical analysis of the phosphorus and ceesium contents in the powder was performed using inductively-coupled plasma atomic emission spectrometry (ICP-AES) and atomic adsorption spectrophotometry (AAS), respectively. The molar ratio of Cs/P in the powder as determined by these methods was 1.05 ± 0.05, consistent with the stoichiometry of CsH_2PO_4.

3. Conductivity measurements

For conductivity measurements, the CsH_2PO_4 powder was pressed uniaxially at 2 ton cm^{-2} for 10 min, using a NPa system TB-200H, in the form of pellets with diameter of 1.11 cm, thickness of 3 ± 0.5 mm, and relative density of $95 \pm 2\%$. Silver electrodes were applied to both sides of the pellet with silver paint (Fujikawa Kasei, D-550). The pellet was placed at the end of an alumina tube in a stainless chamber, Fig. 1, and the chamber set horizontally within a tube furnace. The temperature of the pellet was monitored using a chromel–alumel thermocouple placed close to the sample. Humidified Ar gas was flowed at 12 ml min^{-1} (under atmospheric pressure at 20 °C) through the alumina tube, and the pellet was maintained under selected partial pressures of water (p_{H_2O}) in the range of 0.063 to 0.18 atm. The desired humidification levels were obtained by passing the inlet gas through a water bath maintained at an appropriate temperature between 37 and 59 °C. That complete water saturation of the inlet Ar gas had occurred was confirmed by performing selected experiments at several flow rates and observing no difference in the results.

The conductivity of the sample was measured continuously by a.c. impedance spectroscopy while heating at three different heating rates: 1.2, 3.0, and 12 K h^{-1}. Uniformity of the temperature of the pellet and its immediate surroundings was ensured by preheating the incoming gas through silica–alumina wool that filled up the alumina tube. Impedance data were collected using a Solartron 1260 impedance analyzer in the frequency range of 10 Hz to 1 MHz with a voltage amplitude of 100 mV. The measured spectra were plotted in the complex plane (Nyquist representation) to determine the equivalent d.c. conductivity of CsH_2PO_4. Low temperature data, which displayed visible arcs when so plotted, were modeled by an equivalent circuit representation using the commercial software package Z-View. The high temperature data were analyzed by simple extrapolation of the straight line data to the intercept with the real axis.

Fig. 2 shows the representative impedance spectra of CsH_2PO_4 obtained under $p_{H_2O} = 0.087$ atm (equivalent to

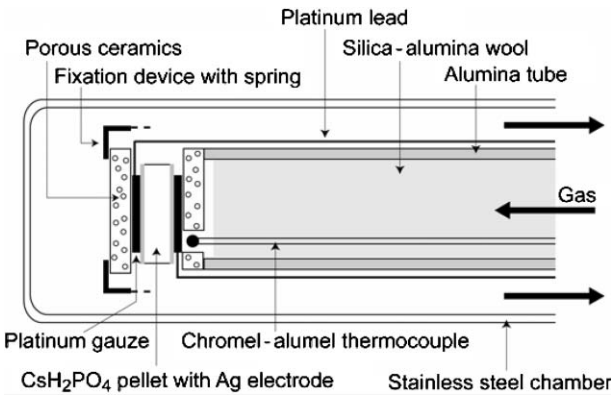

Fig. 1 Schematic diagram of the experimental apparatus used for the conductivity measurements.

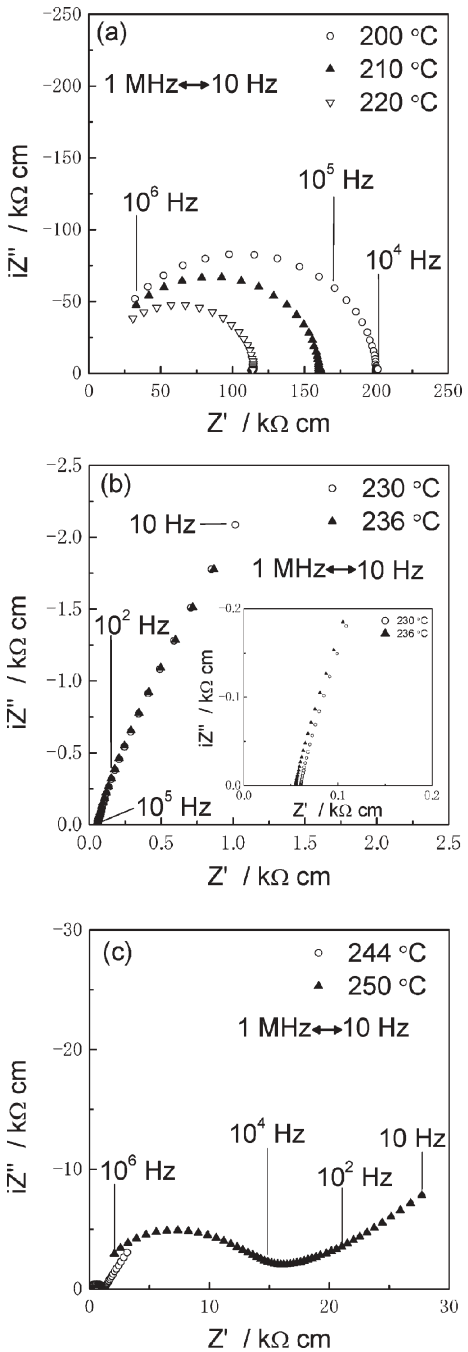

Fig. 2 Typical impedance spectra under $p_{H_2O} = 0.087$ atm at a heating rate of 1.2 K h^{-1}: (a) paraelectric phase; (b) superprotonic phase. Inset is a zoom of high frequency region; (c) mixture of dehydrated products and CsH_2PO_4.

100% humidity at 43.3 °C) and a heating rate of 1.2 K h^{-1}. The spectra collected at 200, 210 and 220 °C, Fig. 2(a), correspond to the non-superprotonic (paraelectric) phase; those collected at 230 and 236 °C, Fig. 2(b), to the superprotonic phase; and those collected at 244 and 250 °C, Fig. 2(c), to the partially dehydrated compound. Abrupt changes in conductivity at the polymorphic and dehydration transformations are evident in Fig. 3, a plot of the conductivity as a function of temperature. The superprotonic phase transition occurs at 228 °C, in agreement with reported values,[3,4] with the conductivity increasing from about 10^{-5} to 10^{-2} S cm^{-1}. As shown in Fig. 3, the conductivity of CsH_2PO_4 remains high until 238 °C, beyond which it monotonically decreases. As already stated, this is taken to reflect the commencement of the dehydration of CsH_2PO_4 and, thus, the temperature at which an abrupt reduction in conductivity was observed is defined as the onset temperature of dehydration (T_{dehy}).

A summary of the results obtained under the three different heating rates and the range of p_{H_2O} is presented in Fig. 4(a), in which the logarithmic values of p_{H_2O} are plotted against the inverse values of T_{dehy}. A distinct linear (Arrhenius) relationship is clearly evident for each of the heating rates. The fact that the data do not coincide for different heating rates, with T_{dehy} decreasing with decreasing heating rate (at a given p_{H_2O}), indicates that the dehydration process is slow such that finite heating rates induce dehydration at temperatures higher than the true equilibrium value. The effect is particularly pronounced at low dehydration temperatures (and low p_{H_2O}) with the apparent T_{dehy} differing by as much as 10 °C between the different heating rates (at a given p_{H_2O}). Thus, further analysis was performed to establish the true equilibrium dehydration temperature.

It has been suggested that during the dehydration of the homologous solid acid of KH_2PO_4 the dehydrated product coats the surface of the unreacted particle and limits further dehydration.[15] It is reasonable to assume that the dehydration of CsH_2PO_4 occurs similarly, with slow diffusion of gas-phase H_2O through the product layer limiting the rate of

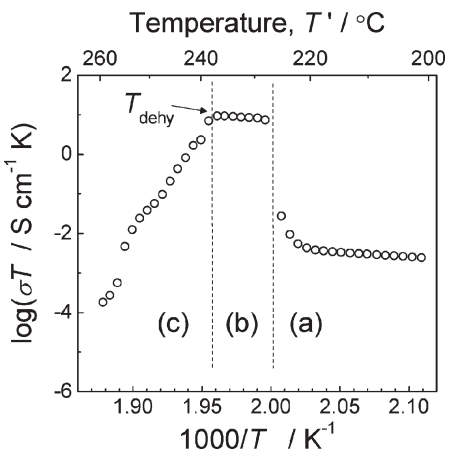

Fig. 3 Temperature dependence of conductivity, σ, of CsH_2PO_4 under p_{H_2O} = 0.087 atm at the heating rate of 1.2 K h^{-1}: (a) paraelectric phase; (b) superprotonic phase; (c) mixture of dehydrated products and CsH_2PO_4.

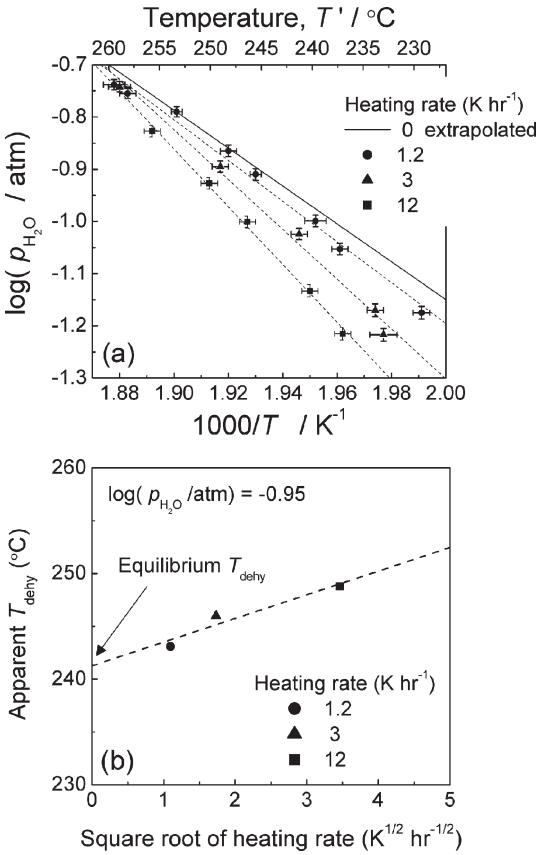

Fig. 4 (a) Onset temperature of dehydration of CsH_2PO_4 under various humidity conditions and at various heating rates. (b) Extrapolation of the onset temperatures of dehydration at $\log(p_{H_2O}) = -0.95$ to the heating rate of zero. Onset temperatures of dehydration are assumed to be proportional to the square root of the heating rate.

transformation of the un-reacted shrinking core. It can be shown for such a process that the lag, ΔT, in the dehydration temperature from its equilibrium value is proportional to the square root of the heating rate. Thus, T_{dehy} can be plotted, for a given p_{H_2O}, as a function of square root of the heating rate, and extrapolation to zero heating rate yields the equilibrium value of T_{dehy}. In the matrix of experiments performed here, the sets of p_{H_2O} used for each of the three heating rates were not exactly identical. Thus, in order to perform the analysis, the implied Arrhenius behavior displayed in Fig. 4(a) was used to interpolate and obtain T_{dehy} for a set of five values of p_{H_2O}. With these values in hand, it was possible to plot the apparent T_{dehy} against the square root of heating rate at a p_{H_2O}; an example of the analysis is presented in Fig. 4(b) for $\log(p_{H_2O}/\text{atm}) = -0.95$. A reasonably linear relationship is apparent in the data, and an equilibrium value of T_{dehy} could be determined by extrapolation to zero heating rate. The procedure was repeated for the five selected values of p_{H_2O}. The resultant relationship between T_{dehy} and p_{H_2O} is represented as a solid line in Fig. 4(a) and is numerically described as:

$$\log(p_{H_2O}/\text{atm}) = 6.11(\pm 0.82) - 3.63(\pm 0.42) \times \frac{1000}{T_{dehy}} \quad (1)$$

4. Thermogravimetric analysis

Thermogravimetric analysis (TGA) of powdered CsH_2PO_4 was carried out using two different systems, the first being a commercial instrument, Rigaku TG-DTA/HUM, and the second being an in-house constructed system that enabled access to higher values of p_{H_2O} than possible with standard commercial instruments. In the case of the commercial system, the measurement was carried out under Ar, humidified to the desired level, and supplied at a flow rate of 400 ml min^{-1}. Sample weight was typically $\sim$40 mg, and platinum containers were utilized. The accuracy in the weight loss measurements was about $\pm$0.5 wt%. The configuration of the in-house constructed system is shown in Fig. 5. It consists of an oven in which a water bath and a sample in a platinum crucible, hanging onto an exterior electronic balance, are placed. The atmosphere surrounding the sample is suitably humidified static air. An additional heater around the sample maintains the temperature and therefore the uniformity of the humidity in the vicinity of the sample. A platinum–platinum/rhodium thermocouple placed close to the internal heater is used for controlling the temperature and another is embedded directly into the sample for monitoring its behavior. In addition, a humidity sensor is placed close to the sample. The accuracy of the weight was $\pm$2 mg, implying, for a typical sample weight of 0.5 g, that the accuracy in the weight loss measurements is $\pm$0.4 wt%.

Isothermal weight-change measurements were carried out using the in-house system with the objective of assessing the accuracy of the relationship between T_{dehy} and p_{H_2O} determined from the conductivity measurements. Fig. 6 shows the weight evolution of CsH_2PO_4 powder at selected temperatures under p_{H_2O} = 0.10 and 0.20 atm in panels (a) and (b), respectively. Based on eqn (1), dehydration is anticipated to occur at 237 $\pm$ 1 °C for p_{H_2O} = 0.10 atm and at 260 $\pm$ 3 °C for p_{H_2O} = 0.20 atm. Accordingly, isothermal experiments were performed at just above and just below these respective temperatures: at 235.4 °C and 237.7 °C for p_{H_2O} = 0.10 atm,

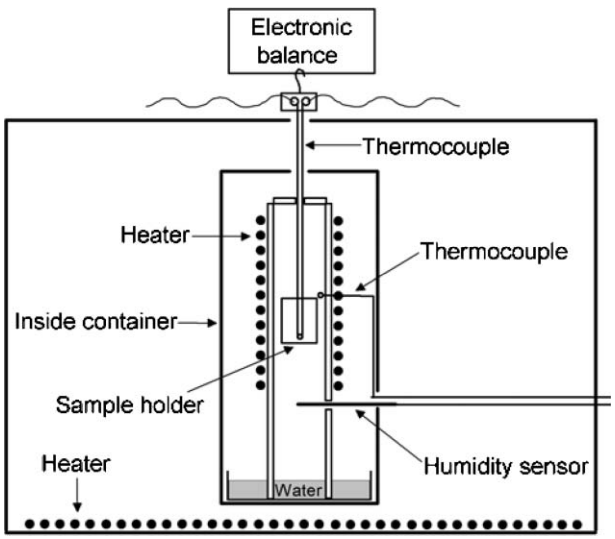

Fig. 5 Schematic diagram of the in-house experimental apparatus used for the thermogravimetric analysis.

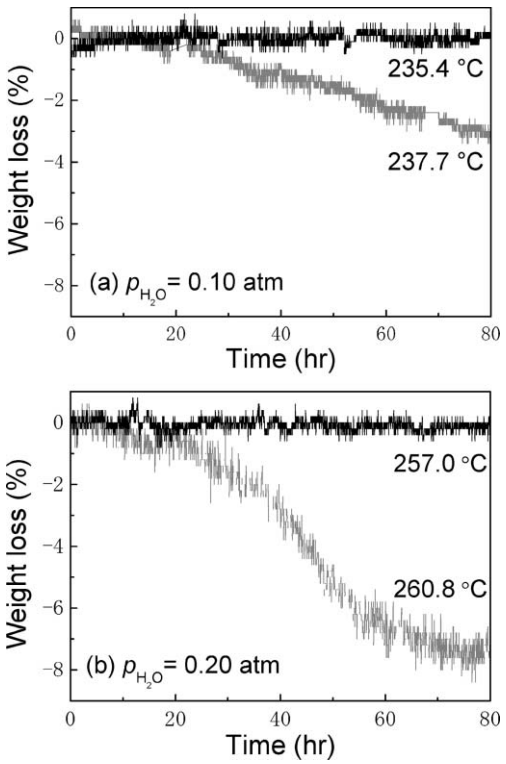

Fig. 6 Thermogravimetric analysis of CsH_2PO_4 powder under the isothermal conditions: (a) at 235.4 and 237.7 °C under p_{H_2O} = 0.10 atm, and (b) at 257.0 and 260.8 °C under p_{H_2O} = 0.20 atm.

and at 257.0 °C and 260.8 °C for p_{H_2O} = 0.20 atm. As summarized in Fig. 7, the results show excellent agreement with eqn (1). Specifically, the sample held at 257.0 °C under p_{H_2O} = 0.20 atm showed no weight change over a period of 80 h, whereas that held at 260.8 °C began to lose detectable amounts of weight after about 10 h, and dehydration was complete after about 80 h. The total weight loss of this sample, 7.3 $\pm$ 0.8%, corresponds well to the theoretical value for the formation of $CsPO_3$, 7.84%. Similarly, the sample held at

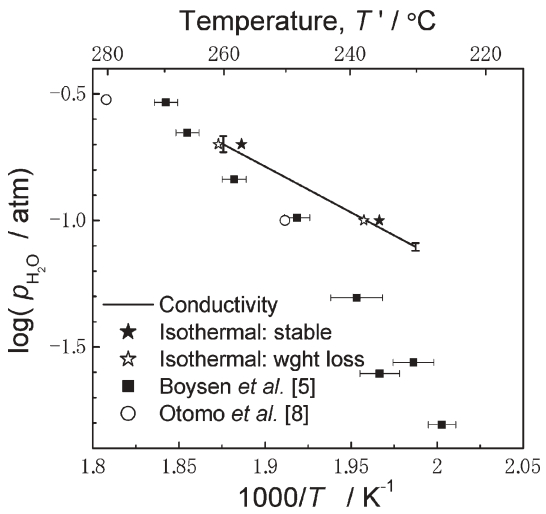

Fig. 7 Comparison of the onset temperatures of dehydration obtained in conductivity measurement and isothermal TGA with those reported by Boysen *et al.*[5] and Otomo *et al.*[8]

235.4 °C under p_{H_2O} = 0.10 atm displayed no weight loss after 80 h, whereas that held at 237.7 °C underwent detectable weight loss after about 20 h. In this case, however, even after 80 h dehydration was not complete, indicating that at lower temperatures the kinetics of the dehydration process is extremely slow. This likely explains the large discrepancy between the earlier dehydration results of Boysen *et al.*[5] and of Otomo *et al.*,[8] also shown for comparison in Fig. 7, who employed finite heating rates (as high as 24 K h^{-1} in the work of Boysen *et al.*[5]).

Thermogravimetric analysis under a fixed heating rate was subsequently performed with the objective of elucidating the dehydration pathway. The sample temperature was increased at the rate of 1 K h^{-1} under p_{H_2O} = 0.095 atm. The results, both in terms of the weight loss (thermogravimetric, TG) and differential weight loss (differential thermogravimetric, DTG) curves, are showed in Fig. 8. The weight loss values corresponding to the formation of the hypothetical intermediate product, $Cs_2H_2P_2O_7$, and the expected final product, $CsPO_3$, 3.92 and 7.84 wt%, respectively, are also shown in Fig. 8(a).

The TG and DTG curves reveal an onset temperature for dehydration of 238.5 ± 1 °C, which, as expected due the finite heating rate, is slightly higher than the equilibrium value implied by eqn (1) , *i.e.*, 236 ± 1 °C. The dehydration reaction concludes at around 258 °C (T_{end} in Fig. 8) and the total weight loss is 7.68% which is in excellent agreement with the theoretical weight loss to form $CsPO_3$. The completely dehydrated product was observed to be a loose powder, indicating that $CsPO_3$ is a solid up to a temperature of 260 °C, and that the dehydration reaction does not, to these temperatures, involve a liquid phase.

Careful examination of these TGA results reveals that although there is no obvious plateau in the weight loss at a value corresponding to the formation of $Cs_2H_2P_2O_7$, the rate

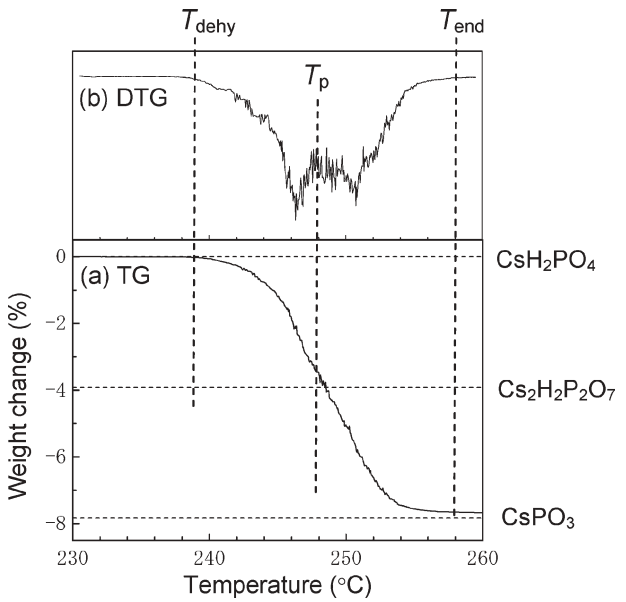

Fig. 8 Thermogravimetric analysis of CsH_2PO_4 powder at the heating rate of 1 K h^{-1} under p_{H_2O} = 0.095 atm: (a) weight change (TG curve); (b) differential values of weight change (DTG curve).

of weight change displays a local minimum at approximately this position. That is, the DTG curve displays a local minimum (in its magnitude) at 248 °C [indicated as T_p in Fig. 8(b)], at which point the weight loss corresponds closely to that for formation of $Cs_2H_2P_2O_7$. Thus, the dehydration reaction under constant heating shows evidence of a two-step process involving the formation of $Cs_2H_2P_2O_7$. This result shows some contrast to the behavior under isothermal conditions, Fig. 6, in which the dehydration appears more continuous.

5. X-Ray powder diffraction analysis of reaction products

In order to determine the nature of the dehydrated product as well as to further elucidate the reaction pathway, X-ray powder diffraction patterns were collected from samples at various levels of dehydration. Diffraction patterns were measured using either a Rigaku 2200 (Cu-K_α, 40 kV, 30 mA) at a scan rate of 0.6° 2θ min^{-1} with an angular resolution of 0.02°, or using an Philips X'Pert Pro (Cu-K_α, 40 kV, 40 mA) at a scan rate of 0.01° 2θ min^{-1} with an angular resolution of 0.017°. Results from five experiments are presented in Fig. 9.

The first pattern, labeled as (1), corresponds to that of fully dehydrated CsH_2PO_4, in which the dehydration was carried out under flowing dry Ar at 240 °C for 60 h. The total weight loss of this sample was 8.0 ± 0.5%, corresponding well to that for the formation of $CsPO_3$ (7.84%). Accordingly, we take this be the reference pattern of caesium metaphosphate. It is noteworthy that this pattern does not match any of those reported for $CsPO_3$ in the JCPDS database (ref #. 37-0027, 38-0135, 43-0096, 43-0101, and 45-0617). We attribute this to the polymorphic behavior of $CsPO_3$, which is known to crystallize in long-chain, cyclic and other forms depending on the details of the thermal history and preparation methods.[15] On the basis of the work of Osterheld and Markowitz,[10] who used the Jones method[16] to analyze the dehydration products of CsH_2PO_4 obtained under similar dry conditions, we conclude that the product phase generated in this study is long-chain $CsPO_3$.

The second pattern, labeled (2) in Fig. 9(a), corresponds to the fully dehydrated product obtained under humidified conditions. Specifically, this pattern was collected from the sample represented in Fig. 7(b), in which dehydration was carried out at 260.8 °C for 85 h under stagnant, humidified air with p_{H_2O} = 0.20 atm (weight loss of 7.3 ± 0.4%). Comparison of patterns (1) and (2) immediately reveals that dehydration under dry conditions and under humid conditions at similar temperatures yields essentially identical product phases.

Patterns (3)–(5) of Fig. 9(a) were obtained from samples that experienced incomplete dehydration. The sample represented by pattern (3) was dehydrated isothermally at 250 °C for 30 h under flowing, humidified Ar with p_{H_2O} = 0.12 atm. The dehydration experiment was performed in a thermal gravimetric analyzer (Rigaku TG-DTA/HUM) and the sample removed and quenched to room temperature in air (to prevent rehydration upon cooling) at the point when the weight loss reached 4.2%, which is just beyond the value expected for the formation of $Cs_2H_2P_2O_7$ (3.92%). The resulting diffraction pattern, Fig. 9(a), pattern (3), clearly shows the presence of

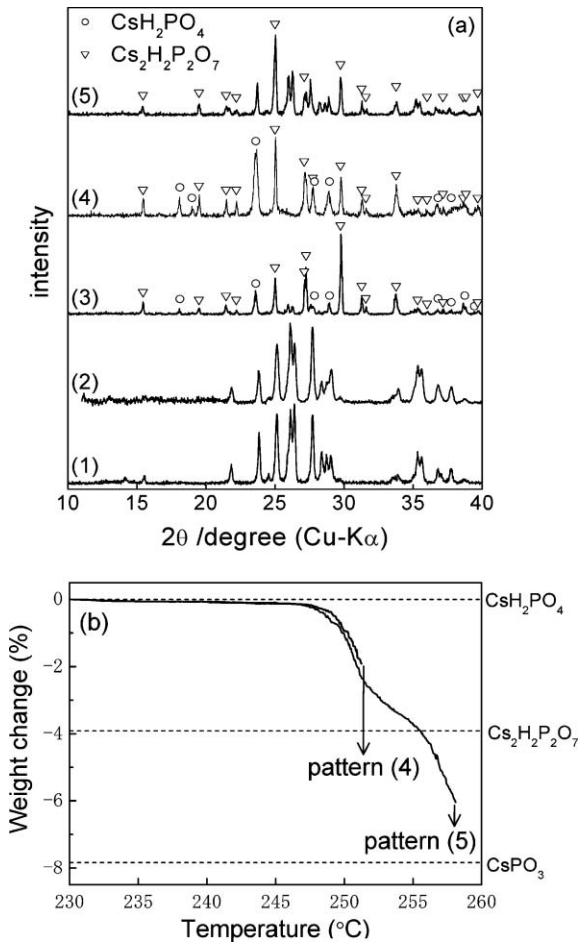

Fig. 9 (a) X-Ray diffraction patterns of CsH_2PO_4 powder dehydrated fully or partially. (1) Fully dehydrated at 240 °C under dry conditions for 60 h. This pattern is used as reference pattern of $CsPO_3$. (2) Fully dehydrated at just above T_{dehy}, *i.e.*, at 260.8 °C under p_{H_2O} = 0.20 atm for 85 h. (3) Partially dehydrated at 250 °C under p_{H_2O} = 0.12 atm for 30 h, where weight loss of sample is 4.2%. (4) Quenched from 251 °C, where weight loss is 1.9%. (5) Quenched from 258 °C, where weight loss is 6.0%. (b) Weight change profile at the heating rate of 1 K h^{-1} under p_{H_2O} = 0.1 atm.

CsH_2PO_4,[14] $Cs_2H_2P_2O_7$[17] and $CsPO_3$, with the pyrophosphate being the dominant phase. Assuming the absence of solid solutions in this system, the Gibb's phase rule implies that only one solid phase should be in equilibrium with H_2O at arbitrary temperature and pressure. Thus, the diffraction pattern must represent non-equilibrium conditions, with $Cs_2H_2P_2O_7$ appearing only as a transient phase. The appearance of this phase suggests that the dehydration of CsH_2PO_4 under isothermal conditions occurs by a two-step process, in which the material first forms $Cs_2H_2P_2O_7$, caesium pyrophosphate, which subsequently dehydrates to form $CsPO_3$, caesium metaphosphate. It is noteworthy that this behavior occurs despite the absence of obvious evidence for a change in the rate of weight loss at values corresponding to pyrophosphate formation, Fig. 6, under isothermal weight loss conditions. The weight loss behavior thus suggests that the two steps of the dehydration are highly overlapping, consistent with the transient nature of $Cs_2H_2P_2O_7$.

The samples for patterns (4) and (5) were prepared by carrying out the dehydration again in a thermal gravimetric analyzer (Rigaku TG-DTA/HUM) at a constant heating rate of 1 K h^{-1}. The atmosphere was again flowing, humidified Ar, in this case with p_{H_2O} = 0.1 atm. The powders were removed from the instrument when the weight loss reached the values of 1.9% and 6.0%, respectively, and were again quenched to room temperature in air. The weight change profiles of each of these two samples are presented in Fig. 9(b). From these data the slowing of the weight loss rate at intermediate values of dehydration is again evident. The diffraction data show that the sample with a weight loss of 1.9% consisted of a mixture of CsH_2PO_4 and $Cs_2H_2P_2O_7$, whereas that with a weight loss of 6.0% consisted of a mixture of $Cs_2H_2P_2O_7$ and $CsPO_3$. These results support the conclusion implied by the TGA data alone, that the dehydration of CsH_2PO_4 under constant heating, just as in the case of isothermal conditions, occurs by a two-step process.

6. Discussion

6.1. Reaction pathway

The isothermal weight change experiments and diffraction patterns obtained from samples allowed to fully equilibrate demonstrate that $CsPO_3$ is the thermodynamically stable phase even at temperatures just above T_{dehy} as measured from the conductivity experiments. From this, it is reasonable to assume that the metaphosphate is the equilibrium phase for all conditions leading to dehydration. The path to $CsPO_3$ formation, however, clearly involves $Cs_2H_2P_2O_7$ under both isothermal and constant heating conditions. Thus, the reaction pathway can be described as

$$CsH_2PO_4 \rightarrow Cs_2H_2P_2O_7 \rightarrow CsPO_3 \quad (2)$$

This observation suggests that the reaction rate to form $Cs_2H_2P_2O_7$ from CsH_2PO_4 is faster than that to form $CsPO_3$ from CsH_2PO_4 or $Cs_2H_2P_2O_7$. This behavior may be a consequence of the structural differences between the three compounds. The transformation from CsH_2PO_4 to $Cs_2H_2P_2O_7$ presumably requires the condensation of pairs of isolated phosphate anions (PO_4^{3-}) to form pyrophosphate anions ($P_2O_7^{4-}$). The transformation to $CsPO_3$, in contrast, requires the coordinated rearrangement of all of the phosphate anions to form the metaphosphate chain, $(PO_3^-)_\infty$. Finally, it is noteworthy that although extensive studies were not carried out to evaluate the possibility of the formation of partially dehydrated products with arbitrary proton content, no evidence was found for the presence of $CsH_{2(1-x)}PO_{4-x}$ species as intermediate phases.

6.2. Assessment of thermodynamic parameter of $CsPO_3$

If one accepts the assumption, justified above, that the line shown in Fig. 7 represents the boundary between phase stability of CsH_2PO_4 and $CsPO_3$, then that boundary reflects the thermodynamics of the reaction

$$C_SH_2PO_4(s,sp) \leftrightarrow CsPO_3(s) + H_2O(g)$$
$$\ln p_{H_2O} = -\Delta_{dehy}G^\circ(T)/RT \quad (3)$$

Table 1 Thermodynamic values used in the thermodynamic evaluation of $CsPO_3$; standard enthalpy, entropy and Gibbs energy of the formation of CsH_2PO_4 and H_2O at 298 K, and enthalpy and entropy of the superprotonic transition of CsH_2PO_4

	Formation properties			
	$\Delta_f H^\circ$/kJ mol^{-1}	$\Delta_f S^\circ$/J mol^{-1} K^{-1}	$\Delta_f G^\circ$/kJ mol^{-1}	Source
CsH_2PO_4(s, pe)	−1564.8	−514.2[a]	−1412	ref. 19, estimated
H_2O(g)	−241.818	−44.427	−228.572	ref. 19

Reaction	$\Delta_{trans}H$/kJ mol^{-1}	$\Delta_{trans}S$/J mol^{-1} K^{-1}	T/K	Source
CsH_2PO_4 (s,pe) → CsH_2PO_4 (s, sp)	11.6 ± 0.6	22.5 ± 1.1	503	ref. 4,20

[a] Estimated in the present work by Latimer's method.[18]

(sp: superprotonic phase) irrespective of the details of the reaction pathway and the transient appearance of $Cs_2H_2P_2O_7$. Eqn (3) can be rewritten as follows:

$$\log p_{H_2O} = \frac{\Delta_{dehy}S^\circ(T_{dehy})}{2.303R} - \frac{\Delta_{dehy}H^\circ(T_{dehy})}{2.303R}\frac{1}{T_{dehy}} \quad (4)$$

Taking the standard enthalpy [$\Delta_{dehy}H^\circ$] and the standard entropy [$\Delta_{dehy}S^\circ$] of the dehydration reaction to be approximately constant in the narrow temperature range of 230 °C to 260 °C (as justified by the results shown in Fig. 7) and inserting the numerical values of eqn (1) into eqn (4) yields:

$$\Delta_{dehy}H^\circ = 69.5 \pm 8.0 \text{ kJ mol}^{-1}$$

$$\Delta_{dehy}S^\circ = 117 \pm 16 \text{ J mol}^{-1} \text{ K}^{-1}$$

These values are in reasonable agreement with those reported earlier by Yaglov *et al.*,[11] 81.5 kJ mol^{-1} and 137.65 J mol^{-1} K^{-1}, respectively.

The $\Delta_{dehy}G^\circ(T_{dehy})$ for reaction (3) is related to the standard Gibbs energy of formation, $\Delta_f G^\circ$, of the reactant and product phases according to:

$$\Delta_{dehy}G^\circ(T_{dehy}) = \Delta_f G^\circ(CsPO_3(s), T_{dehy}) + \Delta_f G^\circ(H_2O(g), T_{dehy}) - \Delta_f G^\circ(CsH_2PO_4(s), T_{dehy}) \quad (5)$$

Thus, from the data derived above and from application of the Neumann and Kopp rule,[18] which states the standard enthalpy and the standard entropy of the dehydration reaction are constant with temperature, it is possible, in principle, to estimate the standard enthalpy [$\Delta_f H^\circ(CsPO_3(s), 298 K)$] and the standard entropy [$\Delta_f S^\circ(CsPO_3(s), 298 K)$] of the formation of $CsPO_3$(s) at 25 °C. Doing so, however, requires knowledge of the thermodynamic properties of H_2O(g) and CsH_2PO_4(s).

While complete thermodynamic data are available in the literature for H_2O(g),[19] the same is not true of CsH_2PO_4(s). For this compound, the standard enthalpy [$\Delta_f H^\circ(CsH_2PO_4(s), 298 K)$] has been reported,[19] but not the standard entropy of formation [$\Delta_f S^\circ(CsH_2PO_4(s), 298 K)$]. Here, we approximate $\Delta_f S^\circ(CsH_2PO_4(s), 298K)$ by Latimer's method,[18] which allows the estimation of the entropy of an ionic solid from the sum of the entropy of the component ions. The entropy of the $H_2PO_4^-$ anion was, in turn, estimated from the properties of other alkali metal dihydrogen phosphates, NaH_2PO_4 and KH_2PO_4, and that of the caesium cation from Latimer's table.[18] Because the dehydration of CsH_2PO_4 has been measured here from the superprotonic phase, CsH_2PO_4(s,sp), but at 25 °C the compound exists in the paraelectric phase, CsH_2PO_4(s,pe), it is further necessary to take into account the enthalpy and entropy changes occurring at the superprotonic transition in order to evaluate the properties of $CsPO_3$(s) from eqn (5). These values are available from the literature.[4,20] Thus, all of the thermodynamic data required for the analysis are either available in the literature or can be estimated. The values used are summarized in Table 1.

The resulting values obtained for the standard enthalpy, standard entropy and standard Gibbs energy, $\Delta_f H^\circ(CsPO_3(s), 298 K)$, $\Delta_f S^\circ(CsPO_3(s), 298 K)$, and $\Delta_f G^\circ(CsPO_3(s), 298 K)$, respectively, of the formation $CsPO_3$ are presented in Table 2. The results are compared to literature data for KPO_3 and $RbPO_3$, as well as earlier data for $CsPO_3$.[19] The value of $\Delta_f H^\circ(CsPO_3(s), 298 K)$ determined in the present study, −1242 ± 9 kJ mol^{-1}, is virtually identical to the previously reported value of −1241.4 kJ mol^{-1}, although some caution is required in making such a comparison because the crystalline phase of $CsPO_3$(s) to which the literature data apply is not known. As further indicated in Table 2, the value of $\Delta_f S^\circ(CsPO_3(s), 298 K)$ is comparable to that of KPO_3, although again, there is uncertainty in this comparison because of the unknown crystal structures. Nevertheless, the good agreement between the thermodynamic values estimated here for the formation of $CsPO_3$(s) and previous results suggests that the dehydration relationship, eqn (1) indeed represents the boundary between CsH_2PO_4 and $CsPO_3$ phase stability.

7. Conclusion

In this study, we investigated the dehydration behavior of CsH_2PO_4 in the temperature range of 230 °C to 260 °C, an important range for SAFC operation. Our results can be summarized as follows:

Table 2 Standard enthalpy, entropy, and Gibbs energy of the formation of $CsPO_3$ at 298 K. Estimated values was compared with the values reported in literature[19]

	$\Delta_f H^\circ$/ kJ mol^{-1}	$\Delta_f S^\circ$/ J mol^{-1} K^{-1}	$\Delta_f G^\circ$/ kJ mol^{-1}	Source
$CsPO_3$(s)	−1242 (±9)	−330 (±17)	−1144 (±14)	This study
KPO_3(s)	—	−304.49	—	Literature[19]
$RbPO_3$(s)	−1237.2	—	—	
$CsPO_3$(s)	−1241.4	—	—	

(1) In the region of interest, the relationship between the onset temperature of dehydration (T_{dehy}) and the partial pressure of water (p_{H_2O}) is expressed by the equation:

$$\log(p_{H_2O}/\text{atm}) = 6.11(\pm 0.82) - 3.63(\pm 0.42) \times \frac{1000}{T_{dehy}}$$

(2) The corresponding dehydration reaction is:

$$CsH_2PO_4(s,sp) \rightarrow CsPO_3(s) + H_2O(g)$$

(sp : superprotonic phase)

(3) The standard enthalpy and the standard entropy of the dehydration reaction of $C_SH_2PO_4(s,sp) \rightarrow CsPO_3(s) + H_2O(g)$ are as follows:

$$\Delta_{dehy}H^\circ = 69.5 \pm 8.0 \text{ kJ mol}^{-1}$$

$$\Delta_{dehy}S^\circ = 117 \pm 16 \text{ J mol}^{-1} \text{ K}^{-1}$$

Furthermore, the standard Gibbs energy of formation of $CsPO_3(s)$ at 25 °C was evaluated:

$$\Delta_f G^\circ(C_SPO_3(s), 298 \text{ K}) = -1144 \pm 14 \text{ kJ mol}^{-1}$$

(4) Mechanistically, the reaction proceeds *via* an initial dehydration to form primarily $Cs_2H_2P_2O_7$, followed by further dehydration to form the final product phase, $CsPO_3$. The pyrophosphate appears only as a transient phase with no detectable regime of thermodynamic stability within the water partial pressure and temperature ranges explored.

Acknowledgements

This work was supported in part by the Sumitomo Foundation and by the U.S. National Science Foundation (DMR-0435221).

References

1 A. I. Baranov, V. P. Khiznichenko, V. A. Sandler and L. A. Shuvalov, *Ferroelectrics*, 1988, **81**, 1147.
2 W. Bronowska, *J. Chem. Phys.*, 2001, **114**(1), 611.
3 J. Otomo, N. Minagawa, C. Wen, K. Eguchi and H. Takahashi, *Solid State Ionics*, 2003, **156**, 357.
4 D. A. Boysen, S. M. Haile, H. Liu and R. A. Secco, *Chem. Mater.*, 2003, **15**, 727.
5 D. A. Boysen, T. Uda, C. R. I. Chisholm and S. M. Haile, *Science*, 2004, **303**, 68.
6 T. Uda and S. M. Haile, *Electrochem. Solid-State Lett.*, 2005, **8**(5), A245.
7 T. Uda, D. A. Boysen, C. R. I. Chisholm and S. M. Haile, *Electrochem. Solid-State Lett.*, 2006, **9**(6), A261.
8 J. Otomo, T. Tamaki, S. Nishida, S. Wang, M. Ogura, T. Kobayashi, C. -J. Wen, H. Nagamoto and H. Takahashi, *J. Appl. Electrochem.*, 2005, **35**, 865.
9 K.-S. Lee, *J. Phys. Chem. Solids*, 1996, **57**(3), 333.
10 R. K. Osterheld and M. M. Markowitz, *J. Phys. Chem.*, 1956, **60**, 863.
11 V. N. Yaglov, P. K. Rud'ko and G. I. Novikov, *Russ. J. Phys. Chem.*, 1972, **46**(2), 310.
12 W. Bronowska and A. Pietraszko, *Solid State Commun.*, 1990, **76**, 293.
13 D. A. Boysen, *Superprotonic Solid Acids: Structure, Properties, and Applications*, PhD thesis, California Institute of Technology, 2004.
14 JCPDS File Card No. 84-0122, Joint Committee on Powder Diffraction Standards, Swarthmore, PA.
15 E. Thilo, *Condensed Phosphates and Arsenates, in Advances in Inorganic Chemistry and Radiochemistry*, ed. H. J. Emeleus and A. G. Sharpe, Academic Press Inc., New York, 1962, vol. 4, pp. 1–75.
16 L. T. Jones, *Ind. Eng. Chem., Anal. Ed.*, 1942, **14**, 536.
17 JCPDS File Card No. 81-1576, Joint Committee on Powder Diffraction Standards, Swarthmore, PA.
18 O. Kubaschewski and C. B. Alcock, *Metallurgical Thermochemistry*, 5th edn, Pergamon Press Ltd, Oxford, UK, 1979, pp. 184, 189–191.
19 D. D. Wagman *et al.*, *J. Phys. Chem. Ref. Data, Suppl.*, 1982, **11**(2).
20 S. M. Haile, C. R. I. Chisholm, D. A. Boysen, K. Sasaki and T. Uda, *Faraday Discuss.*, 2007, **134**, 17.